IEEE Access
Multidisciplinary | Rapid Review | Open Access Journal

Received September 2, 2020, accepted September 6, 2020, date of publication September 9, 2020,
date of current version September 24, 2020.

Digital Object Identifier 10.1109/ACCESS.2020.3023012

Research on the Applicability of the E Spectrum and PM Spectrum as the First Guess Spectrum of SAR Wave Spectrum Inversion

YONG WAN[1], RUOZHAO QU[2], YONGSHOU DAI[1], AND XIAOYU ZHANG[1]
[1]College of Oceanography and Space Informatics, China University of Petroleum, Qingdao 266580, China
[2]College of Control Science and Engineering, China University of Petroleum, Qingdao 266580, China

Corresponding author: Yong Wan (wanyong@upc.edu.cn)

This work was supported in part by the National Key Research and Development Program of China under Grant 2017YFC1405600.

ABSTRACT Synthetic aperture radar (SAR) is an important method for observing ocean waves, and inversion of the ocean wave spectrum is an important part of SAR ocean wave detection. For most wave spectrum inversion methods, the first guess spectrum is crucial to the accuracy of SAR wave spectrum inversion. The first guess spectrum can be provided by some existing fixed wave spectrum models, but the applicability of these wave spectrum models as the first guess spectrum has not been systematically studied. This paper focused on the applicability of the Elfouhaily spectrum (E spectrum) as a full wavenumber spectrum and the Pierson-Moscowitz spectrum (PM spectrum) as a wind wave spectrum as the first guess spectrum for inverting the wave spectrum. Based on the SENTINEL-1A and RADARSAT-2 SAR satellite data of the Maritime Silk Road, using the E spectrum and PM spectrum as the first guess spectrum by the Max Planck Institute (MPI) method, the ability of the E spectrum and PM spectrum as the first guess spectrum to retrieve the wave spectrum and wave parameters was systematically evaluated. The significant wave height (H_S) and zero-crossing period (T_Z) wave parameters obtained from SAR inversion were compared with the European Center for Medium-Range Weather Forecasts (ECMWF) wave data. By the comparison results, we analyzed the best wind speed and significant wave height ranges for the inversion of the PM spectrum and E spectrum as the first guess spectrum. The results showed that the E spectrum as the first guess spectrum had a good effect on the inversion at medium sea situation. It was suitable as the first guess spectrum of the SAR wave spectrum inversion.

INDEX TERMS SAR, wave spectrum inversion, MPI method, E spectrum, PM spectrum, applicability, maritime silk road.

I. INTRODUCTION

Ocean waves are an important marine dynamic process. They are small-scale wind-generated gravity waves that occur on the ocean surface, including wind waves and swells. Studying the generation and evolution mechanism of ocean waves has become an important research area in physical oceanography. Monitoring waves is of great significance for the construction and security of national defense, shipping, shipbuilding, ports, and offshore oil platforms. Additionally, waves are also important targets for global marine environmental monitoring and global climate research.

The 21st Century Maritime Silk Road is an important part of the Belt and Road Initiative. Its construction will promote the economic, trade, and cultural development of China and the countries along the route with the marine economy as a breakthrough under the new situation of economic globalization [1]. However, the ability of ocean-going ships to withstand various disasters when sailing along the Maritime Silk Road is relatively weak. The harsh marine environment, such as large waves at sea, will cause considerable damage to marine activities such as marine scientific research, resource exploration, ocean fishery, military activities, and ocean transportation. The damage will seriously affect the safety of ship navigation and maritime activities. Therefore, sea-related activities in the sea areas along the route have urgent demands for the protection of the marine environment and the wave information monitoring [2]. Zheng and his team had carried out a lot of research work on waves and wave energy on the Maritime Silk Road [3]–[6].

The associate editor coordinating the review of this manuscript and approving it for publication was Wenming Cao.

At present, the means for obtaining statistical parameters of ocean waves include ocean wave buoy observations, ocean wave numerical model predictions, and remote sensing observations (SARs). Wave buoy observation is currently recognized as the most accurate method for obtaining wave parameters. It can obtain accurate wave data through observations and can be used in complex marine environments [7]. However, it is difficult for buoy observations to complete the measurement of ocean wave parameters over a wide range, so it is not an ideal method for achieving ocean wave observations over a large area. In addition, the wave numerical prediction model is another important method for obtaining wave parameters. It is widely used to understand and analyze the law of wave generation, propagation, and development, and it is also the main method for wave forecasting and analysis [8]. However, the model results are the results of numerical calculations, not the results of on-site observations. Additionally, the prediction accuracy is affected by many factors, such as the accuracy of the driving wind field, the setting of first conditions, and the assimilation of observation data. Thus, the wave numerical prediction model is also not an ideal method for obtaining wave information.

The development of synthetic aperture radar has provided a new method for ocean wave observation. SAR is an important spaceborne sensor that can provide two-dimensional information about waves, independent of weather and lighting conditions. The spatial resolution of SAR is higher than that of other ocean wave acquisition methods, and the echoes in the resolution unit are not easily affected by land [9]. Using the two-dimensional sea surface images obtained by SAR, the two-dimensional directional spectrum of the waves can be obtained by inversion, which can be used to calculate important wave parameters such as significant wave height, average wave period, and wave propagation direction [10]. Therefore, SAR is an ideal method for long-term ocean wave observations over a wide range.

After years of development, researchers have proposed a variety of SAR wave spectrum inversion methods. Hasselmann and Hasselmann [11] derived a nonlinear transformation from the SAR image spectrum to the wave direction spectrum, and based on this transformation, they developed an MPI algorithm for inverting the wave direction spectrum from the SAR image spectrum. He [12] proposed a parametric wave spectrum inversion method. The core idea was also based on Hasselmann's nonlinear mapping theory. The difference is that the wave spectrum is parameterized when constructing the value function of the inversion algorithm. Mastenbroek and De-Valk [13] proposed a semiparametric method (SPRA) for ocean wave spectrum inversion. During the inversion of this method, the first guess spectrum is not the wave spectrum obtained by the model, but the wind wave spectrum estimated by the wind vector information observed by the scatterometer. Engen and Johnsen [14] proposed an algorithm for obtaining cross-spectra from SAR complex data. This algorithm is a better method for inverting ocean wave direction spectra from SAR images. This method can resolve the 180° ambiguity in the wave propagation direction and can reduce speckle noise, and it is not necessary to obtain the first guess information from the model or other sensors so that the SAR becomes a sensor that can independently observe two-dimensional wave information. Schulz-Stellenfleth *et al.* [15] proposed an improved nonlinear inversion algorithm (PARSA). This method is a combination of the MPI mode and the cross-spectrum algorithm, which solves the problem of 180° ambiguity of ocean wave propagation direction. This method is more accurate than the cross-spectrum method but still needs to provide first guess information.

From the above inversion methods, it can be seen that the problem of 180° ambiguity of the wave propagation direction is still the key problem for the inversion of the spaceborne SAR wave spectrum. At present, the main solution is to use prior information, such as the first guess spectrum [16]. The quality of the first guess spectrum will directly determine the accuracy of the inversion result of the wave spectrum. The first guess spectrum is generally provided by a third party, mainly from the wave numerical prediction model or the classic wave spectrum (PM spectrum, E spectrum, etc.) [17]. Among them, the operation process of the wave numerical prediction model is time consuming [18], and the model is the result of numerical simulation; its accuracy is restricted by many factors. The classic ocean wave spectrum is the ocean wave spectrum obtained by on-site observation, and the ocean wave direction spectrum can be obtained on the basis of the frequency spectrum. Thus, the classic wave spectrum is also an important method for providing the first guess spectrum for SAR wave inversion.

The classic wave spectrum mainly includes the PM spectrum, JONSWAP spectrum, and E spectrum. The PM spectrum is the earliest model of the ocean wave spectrum. It is based on relatively sufficient observation data and describes a fully growing wind wave [19]. The JONSWAP spectrum is an international standard wave spectrum proposed on the basis of the "Joint North Sea Wave Project" system measurements performed in Germany, the United Kingdom, the United States, and the Netherlands from 1968 to 1970 [20]. It is an empirical spectrum obtained from the analysis and fitting of measured wave data, and it is the most systematic and highly accurate wave spectrum [21]. The E spectrum is a universally applicable ocean spectrum model, which is based on the classic ocean wave spectrum JONSWAP, PM spectrum and other spectral models [22]. The E spectrum is a full wavenumber spectrum and a non-empirical ocean spectrum. However, there are currently no systematic studies on the applicability of the PM spectrum and E spectrum as the first guess spectrum of SAR wave spectrum inversion. Therefore, this paper used the E spectrum and PM spectrum as the first guess spectrum for SAR wave spectrum inversion and discussed the applicability of two wave spectrum models as the first guess spectrum for SAR wave spectrum inversion. The research results provide a basis for the selection of the first guess spectrum of SAR

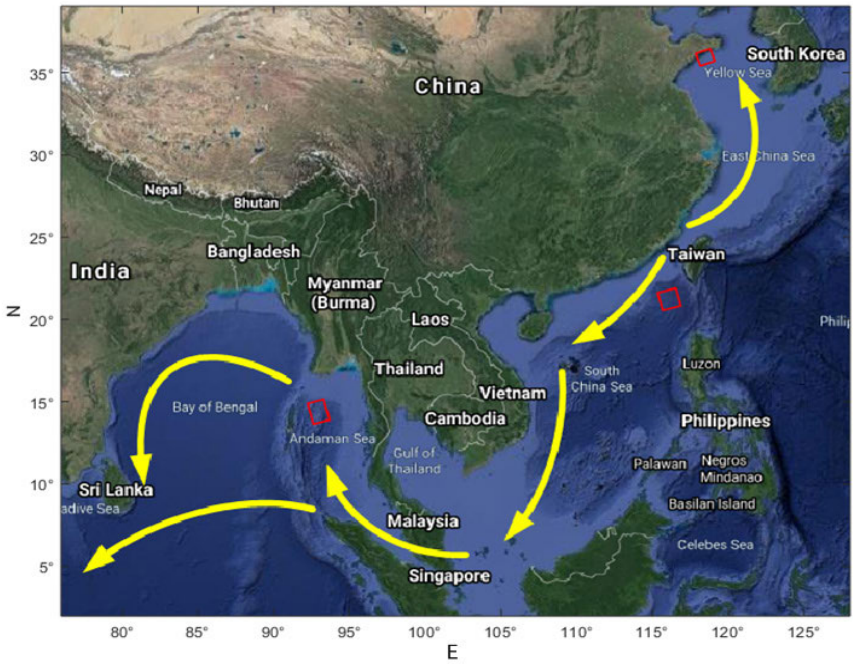

FIGURE 1. The path of the maritime silk road and the location of the research area.

wave spectrum inversion and provide strong support for SAR observations of the distribution of sea waves on the 21st Century Maritime Silk Road.

II. RESEARCH AREA AND DATA

A. RESEARCH AREA

The Maritime Silk Road is an important channel for world economic and cultural exchanges. The research area selected in this paper was mainly the Yellow Sea, South China Sea, and Indian Ocean Andaman Sea of the Maritime Silk Road. The research area is shown in the red box in Fig. 1. Among them, the latitude and longitude range of the research area of the Yellow Sea was 35°N-37°N, 119°E-121°E, and the data was from the RADARSAT-2 SAR satellite. The latitude and longitude of the research area of the South China Sea was 20°N-22°N, 117°E-119°E, and the data was from the RADARSAT-2 SAR satellite. The latitude and longitude of the research area in the Andaman Sea was 12°N-14°N, 93°E-95°E, and the data was from the SENTINEL-1A SAR satellite.

B. DATA

The data used in this article include the SENTINEL-1A SAR data provided by the European Space Agency (ESA), the RADARSAT-2 SAR data provided by the Canadian Space Agency (CSA), and model wind field and wave data provided by ECMWF. They are introduced separately below.

1) SENTINAL-1A SAR DATA

SENTINEL-1A is an all-weather radar imaging system. It is the first satellite developed by the European Commission (EC) and the European Space Agency (ESA) for the Copernican Global Earth Observation Project. The SENTINEL-1A C-band imaging system uses four imaging modes (up to 5 m in resolution and 400 km in width), which are strip mode (SM), interferometric wide swath (IW), extra-wide swath (EW) and wave (WV) modes, with dual polarization, short revisit cycles, and rapid production capabilities [23].

In this article, 12 scenes of SENTINEL-1A satellite VV polarization SM mode SAR data and 2 scenes of WV mode SAR data were selected as part of the SAR data source. A quick view of the Sentinel-1A SAR acquired on 09-JUN-2019 21:53:25 (UTC) is shown in the Fig. 2.

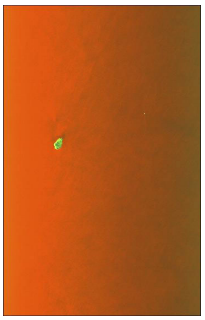

FIGURE 2. A quick view of the Sentinel-1A SAR acquired on 09-JUN-2019 21:53:25 (UTC).

2) RADARSAT-2 SAR DATA

The RADARSAT-2 radar satellite is a C-band synthetic aperture radar launched by the Canadian Space Agency (CSA) on December 14, 2007, which has high spatial resolution imaging capabilities. It can provide radar data with a

resolution of 3 to 100 m, a width of 10 to 500 km, multi-polarization, and multiple resolutions [24].

In this paper, 2 scenes of RADARSAT-2 satellite VV polarized SAR data were selected as a part of the SAR data source. Among them, the SAR image in the Yellow Sea in southwestern Shandong Province was at 25-JUL-2012 22:07:39 (UTC), and the center of the image was 35°47′ 23″N, 120° 28′ 27″E. The SAR image in the South China Sea in the southeast of Taiwan Province was at 23-JUN-2019 21:53:25 (UTC), and the center of the image was 21°30′ 06″N, 118°42′ 26″E. The quick views of this two scenes SAR data are shown in Fig. 3.

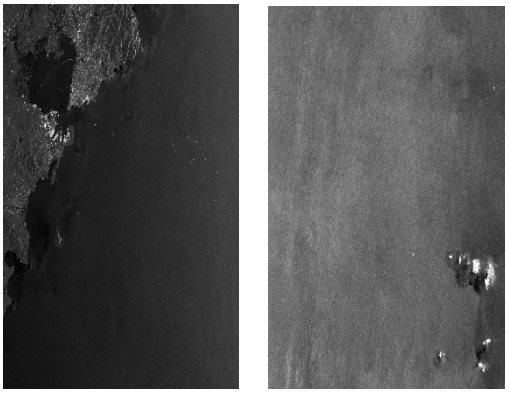

FIGURE 3. The quick views of the Radarsat-2 SAR acquired on 25-JUL-2012 22:07:39 (UTC) and 23-JUN-2019 21:53:25 (UTC).

3) ECMWF DATA

The European Center for Medium-Range Weather Forecasts (ECMWF) can provide global wind field and wave grid data with different spatial resolutions from 1979. The highest spatial resolution is 0.125°×0.125°. The time resolution of the data is six hours, and the corresponding moments are 00:00, 06:00, 12:00, and 18:00.

This paper mainly used the ECMWF ERA-Interim dataset, 10 m wind speed, 10 m wind direction, significant wave height and mean zero-crossing period corresponding to the SAR data observation area and time, with a resolution of 0.125°. The matching time and space windows of ERA-Interim data and SAR data were 120 min and 12.5 km, respectively. Among them, the wind speed and direction provided by ECMWF were used as inputs to construct the first guess spectrum, and the significant wave height and zero-crossing period data were used to verify the accuracy of the wave parameters obtained from the inversion. We obtained 6198 groups of ECMWF data for inversion and verification.

III. SAR WAVE SPECTRUM INVERSION METHODS

A. MPI INVERSION METHOD

Because the transformation between the SAR image spectrum and the ocean wave spectrum is a nonlinear transformation and the SAR image spectrum has 180° direction ambiguity and information loss due to the azimuth cutoff wavenumber, it is difficult to directly obtain the inverse mapping relationship between the SAR image spectrum and ocean wave spectrum. Hasselmann and Hasselmann [11] derived a nonlinear transformation from the SAR image spectrum to the wave direction spectrum and, based on this transformation, developed an MPI algorithm for inverting the wave direction spectrum from the SAR image spectrum. Although the MPI method needs to provide the first guess spectrum, the completeness and accuracy of its inversion information are relatively high under the same conditions. Therefore, this method is used in this paper to realize wave spectrum inversion.

The inversion of the wave spectrum using the MPI method requires inputting the SAR image spectrum and the first guess spectrum and then using forward mapping to calculate the simulated SAR image spectrum from the first guess spectrum. The simulated SAR image spectrum and the observed SAR image spectrum are used to calculate the value function, and then the value function is used to determine whether the iterative process has converged. The definition of the value function is as follows.

$$\mathrm{J}=\int [P(\mathrm{k})-\hat{P}(\mathrm{k})]^{2}\hat{P}(\mathrm{k})\mathrm{dk}+\mu\int \{\frac{[F(\mathrm{k})-\hat{F}(\mathrm{k})]}{[\mathrm{B}+\hat{F}(\mathrm{k})]}\}^{2}\mathrm{dk} \tag{1}$$

where $\hat{F}(k)$ is the first guess spectrum and $F(k)$ is the optimal wave spectrum when J takes the minimum value. $\hat{P}(k)$ and $P(k)$ are the observed SAR spectrum and the optimal SAR spectrum, respectively. μ is the weight coefficient, and the small positive number B is to prevent the value function from being infinite at $\hat{F}(k)=0$.

The value function consists of two parts. One part is the difference between the optimal SAR spectrum and the observed SAR spectrum, and the other part is the difference between the optimal wave spectrum and the first guess spectrum. Minimizing the value function means that the wave spectrum obtained from the inversion is closest to the first guess spectrum, and the simulated SAR image spectrum is also closest to the observed SAR image spectrum. If the value function is smaller than the set small value, it indicates that the process has converged. Otherwise, it is necessary to adjust the wave spectrum, recalculate the simulated SAR image spectrum, and continue to compare with the observed SAR image spectrum to calculate the value function until the process converges or jump out of the iterative process without convergence. The flowchart of the inversion method is shown in Fig. 4.

B. SELECTION OF THE FIRST GUESS SPECTRUM

The selection of the first guess spectrum is important for the accuracy of SAR wave spectrum inversion. We selected the PM spectrum and E spectrum as the first guess spectrum

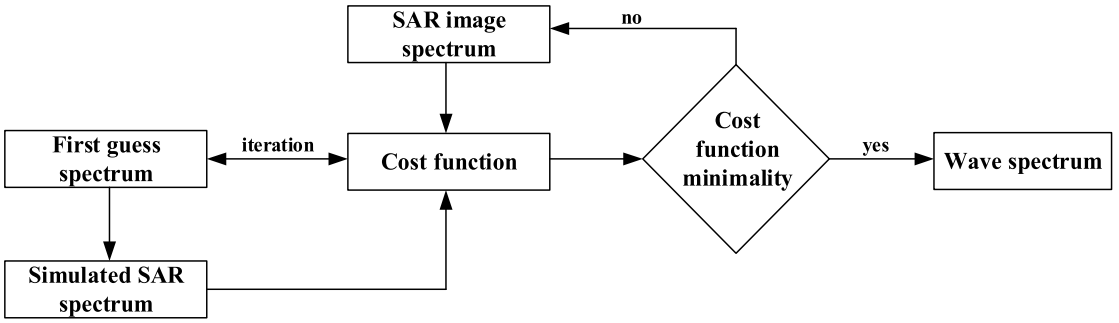

FIGURE 4. Flowchart of the MPI inversion method.

for SAR wave spectrum inversion. The PM spectrum and E spectrum are introduced below.

1) PM SPECTRUM

From 1955-1960, Moscowitz researched observational data obtained from the North Atlantic Ocean, compared and analyzed 54 fully developed wind and wave spectra, and divided them into 5 groups based on wind speed. The final results after averaging had good similarity. Afterward, Pierson and Moscowitz carried out further processing on this basis and obtained the Pierson-Moscowitz spectrum (PM spectrum) of the wavenumber spectrum model of the anchor direction [19]. The PM spectrum belongs to the gravity spectrum and is also a kind of steady-state ocean spectrum. It describes the fully growing wind and waves. It has sufficient observation data as the basis and is also more significant for statistical processing and analysis methods such as dimensionlessness.

The one-dimensional PM spectrum is expressed as follows:

$$S_{PM}(\omega) = \frac{\alpha g^2}{\omega^5} \exp\left[-\beta\left(\frac{g}{U_{19.5}\omega}\right)^4\right] \tag{2}$$

The two-dimensional PM wavenumber direction spectrum is expressed as follows:

$$S_{PM}(k,\phi) = \frac{\alpha}{2k^4}\exp(-\frac{\beta g_0^2}{k^2 U_{19.5}^4})\cdot\frac{2}{\pi}\cos^2(\frac{\phi-\phi_m}{2}) \tag{3}$$

where $\alpha = 0.0081$, $\beta = 0.74$, g is the acceleration of gravity, k is the wavenumber, φ is the wave propagation direction, and φ_m is the main wave direction, usually regarded as the wind direction angle. $U_{19.5}$ is the wind speed at the height of 19.5 m above sea level. However, during the wave calculation process, the wind speed at 10 m above sea level is usually used for calculation. The conversion relationship between wind speeds is as follows [25]:

$$U_h = U_{10}\cdot(1+2.5\lg(\frac{h}{10})) \times(\sqrt{0.0015/[1+\exp\left(-\frac{U_{10}-1.25}{1.56}\right)]+0.00104}) \tag{4}$$

The variation of PM spectrum S(k) with wind speeds is shown in Fig. 5.

2) E SPECTRUM

Elfouhaily *et al*. summarized a universally applicable spectral model based on JONSWAP, PM, and other spectral models [22], referred to as the E spectrum. The E spectrum is a full wavenumber spectrum and a non-empirical ocean spectrum. The spectral model is based on the low wavenumber JONSWAP spectrum [26] and the high wavenumber Phillips spectrum [27]. The key feature of this model is the similarity of description for the high- and low wavenumber regimes; both forms are posed to stress that the air-sea interaction process of friction between wind and waves is occurring at all wavelengths simultaneously. The direction function of the frequency spectrum is symmetrical about the wind direction and has a correlation between wavenumber and wind speed.

The low wavenumber spectrum of the E spectrum is expressed as follows:

$$B_l = \frac{\alpha_p}{2}\cdot\frac{c_p}{c}\cdot F_p \tag{5}$$

where $\alpha_p = 0.006\Omega^{1/2}$ is the equilibrium range parameter for long waves, Ω represents dimensionless inverse wave age, c_p is the phase velocity corresponding to the peak wavenumber, and F_p is the longwave side effect function. The high wavenumber spectrum of the E spectrum is expressed as follows:

$$B_h = \frac{\alpha_m}{2}\cdot\frac{c_m}{c}\cdot F_m \tag{6}$$

where α_m is the equilibrium range parameter for short waves, c_m is the minimum phase velocity, and F_m is the shortwave side effect function.

The full wavenumber spectrum is expressed as follows, and Fig. 6 shows realizations of this omnidirectional spectrum $S(k)$ for several wind speeds.

$$S = k^{-3}(B_l + B_h) \tag{7}$$

The variation of E spectrum S(k) with wind speeds is shown in Fig. 5. The direction function is expressed as follows:

$$f(k,\varphi) = \frac{1}{2\pi}[1+\Delta(k)\cos(2\varphi)] \tag{8}$$

$$\Delta(k) = \tanh[a_0 + a_p(\frac{c}{c_p})^{2.5} + a_m(\frac{c_m}{c})^{2.5}] \tag{9}$$

$$a_0 = \frac{\ln(2)}{4} = 0.1733;\ a_p = 4;\ a_m = 0.13\frac{U_f}{c_m} \tag{10}$$

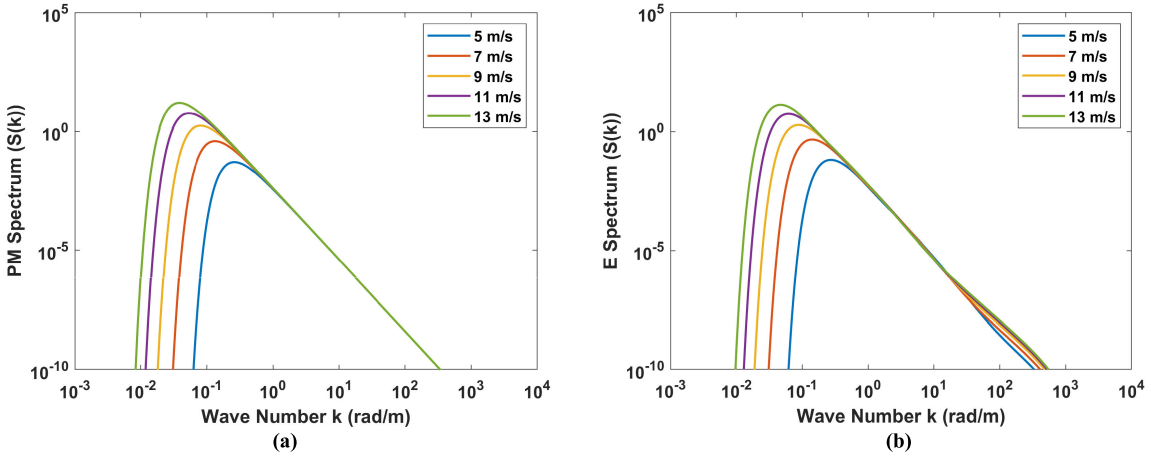

FIGURE 5. PM spectrum S(k) and E spectrum S(k) for the full wavenumber range and for wind speeds from 5m/s up to 13 m/s with a 2 m/s step (a. PM spectrum; b. E spectrum).

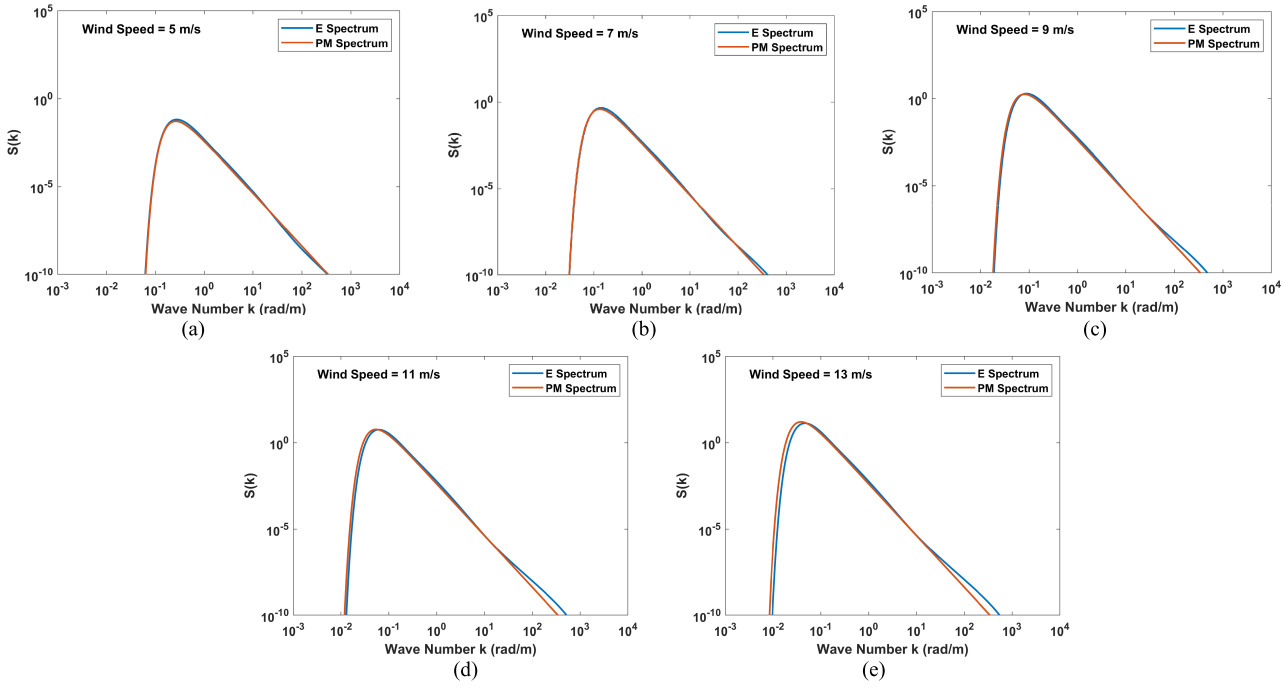

FIGURE 6. E spectrum and PM spectrum S(k) for the full wavenumber range and for different wind speeds (a. 5 m/s; b. 7m/s; c. 9m/s; d. 11m/s; e. 13m/s).

The wavenumber direction E spectrum can be represented by the full wavenumber spectrum and direction function:

$$E(k, \varphi) = S \cdot f(k, \varphi)/k \tag{11}$$

3) COMPARISON OF THE TWO WAVE SPECTRUM

By analyzing the wave spectrum of the E spectrum and PM spectrum for the wavenumber range (Fig. 5), we can see that the E spectrum and PM spectrum are concentrated near the peak of the spectrum, the energy is concentrated, and away from the peak of the spectrum, the energy will drop rapidly. As the wind speed increases, the peak of the sea spectrum will gradually increase, but the peak will move in the direction of a small wavenumber. This indicates that as the wind speed increases, the energy of the sea spectrum increases, and the energy of the waves is more concentrated on long waves with longer wavelengths [28]. In the high wavenumber domain, the PM spectrum does not change significantly with increasing wind speed, and the energy of the short wave of the E spectrum increases with increasing wind speed, which shows that the E spectrum is based on the PM spectrum, and the influence on the short wave is added on the basis of the long wave.

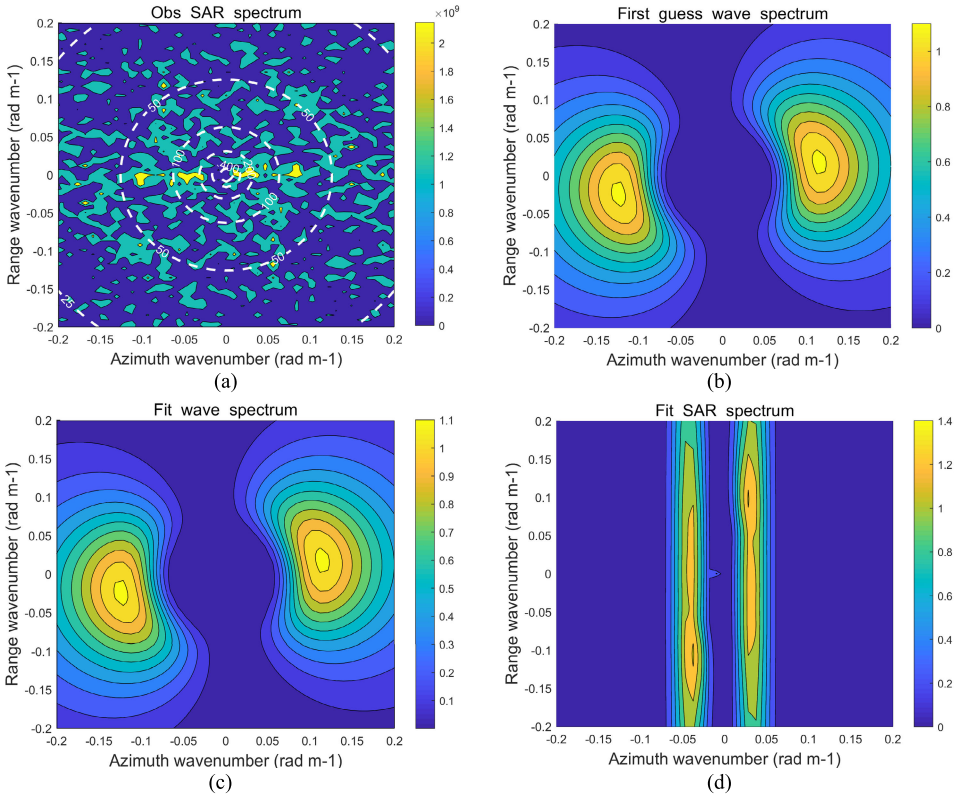

FIGURE 7. Wave spectrum inversion results of 25-JUL-2012 22:07:39 (UTC) RADARSAT-2 SAR data when the E spectrum was used as the first guess spectrum (a. Observed SAR spectrum; b. First guess spectrum (E spectrum); c. Fit wave spectrum; d. Fit SAR spectrum).

Additionally, to analyze the characteristics of the E spectrum and PM spectrum better, we compared the wave spectrum of the E spectrum and PM spectrum with the change in wavenumber according to different wind speeds. As shown in Fig. 6.

From Fig. 6, we can see that in the low wavenumber domain, the E spectrum and the PM spectrum remained basically the same as the wind speed increased. In the high wavenumber domain, as the wind speed increased, the energy of the short wave of the E spectrum gradually increased and moved in the direction of the large wavenumber. When the wind speed was 5 m/s, the curves of the two spectra basically overlapped. When the wind speed increased to 7 m/s, the influence of the E spectrum on short waves began to increase. When the wind speed was approximately 9 m/s or higher than 9 m/s, the E spectrum covered a wider wavenumber domain, and the short wave energy increased significantly. It shows that the E spectrum contains more sea wave information than the PM spectrum.

Therefore, the E spectrum is a full wavenumber spectrum and contains more wave information under high wind speed conditions, and it can be suitable for inversion of various sea wave types and wind speeds. However, the spectral shape of the PM spectrum is relatively stable [29], and the PM spectrum is not sensitive to changes in short waves in the high wavenumber domain, so it is not suitable for the inversion of many complex sea situations with high wind speeds.

IV. APPLICABILITY OF THE PM SPECTRUM AND E SPECTRUM AS THE FIRST GUESS SPECTRUM FOR SAR WAVE SPECTRUM INVERSION

A. DETERMINATION OF THE OPTIMAL FIRST GUESS SPECTRUM MODEL FOR SAR WAVE SPECTRUM INVERSION

In this section, based on the SAR data of the SENTINEL-1A and RADARSAT-2 satellites, the MPI method was used to invert the wave spectrum and wave parameters with the E spectrum and the PM spectrum as the first guess spectrum. By comparing the ability of the E spectrum and PM spectrum as the first guess spectrum to invert the ocean wave spectrum and wave parameters, the optimal first guess spectrum model for SAR ocean wave spectrum inversion was determined. To evaluate the accuracy of the inversion results of wave parameters, we compared it with the ECMWF ERA-Interim wave data.

The MPI method needs to provide the first guess spectrum when retrieving the wave spectrum. When constructing the first guess spectrum, we used the ERA-Interim wind field data as the input wind speed and direction of the first guess spectrum.

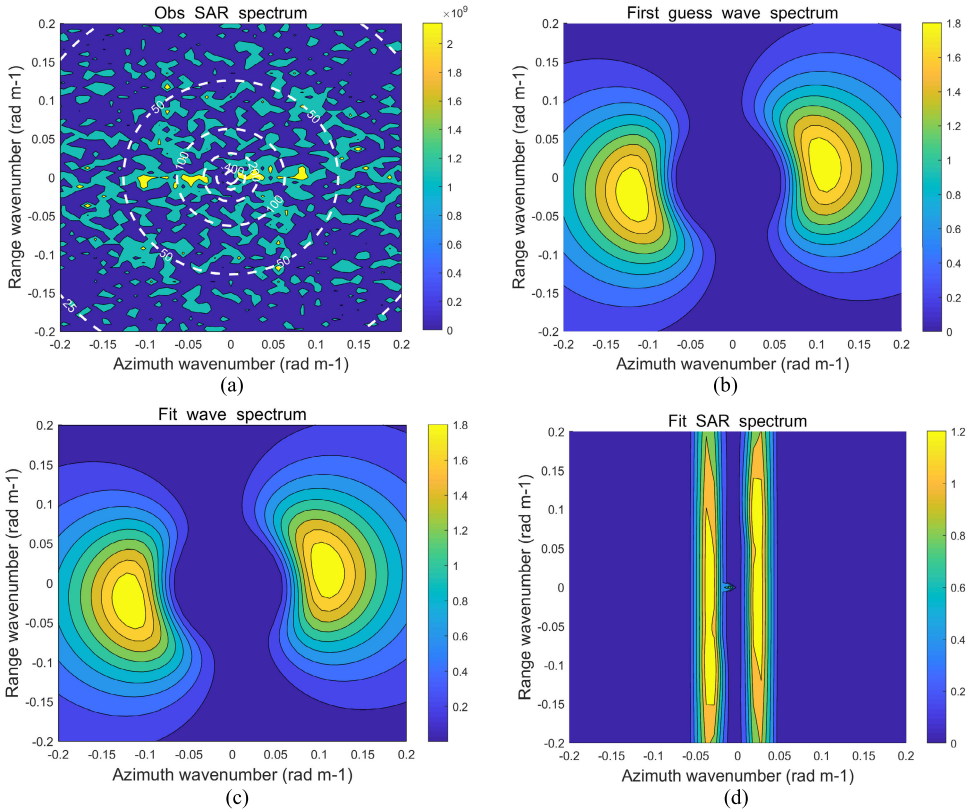

FIGURE 8. Wave spectrum inversion results of 25-JUL-2012 22:07:39 (UTC) RADARSAT-2 SAR data when the PM spectrum was used as the first guess spectrum (a. Observed SAR spectrum; b. First guess spectrum (PM spectrum); c. Fit wave spectrum; d. Fit SAR spectrum).

In this paper, a total of 16 scenes of the SENTINEL-1A satellite and RADARSAT-2 satellite were selected. The intensity data of each SAR image were divided into 20 × 20 small blocks, for a total of 400 sub-images. The intensity data of each sub-image were subjected to fast Fourier transform in units of 128 × 128 pixels to obtain the SAR image spectrum. Then, we used the MPI method to invert the ocean wave spectrum, input the PM spectrum and the E spectrum as the first guess spectrum, calculated the value function and iterated to obtain the fit wave spectrum and the fit SAR spectrum.

Figs. 7-10 show the wave spectrum inversion results with the PM spectrum and E spectrum as the first guess spectrum using two sub-images as an example selected from the RADARSAT-2 and SENTINEL-1A SAR data.

In the wave spectrum inversion results, the observed SAR spectrum was the intensity spectrum after two-dimensional Fourier transform. The fit wave spectrum and the fit SAR spectrum were the results of iteration through the MPI algorithm.

In addition, it was necessary to further calculate the wave parameters from the wave spectrum, such as the significant wave height (H_S) and zero-crossing period (T_Z). Then, we can evaluate the applicability of the first guess spectrum by inverting the accuracy of the obtained wave parameters. The wave spectrum $S(\omega)$ was obtained by integrating the two-dimensional wave direction spectrum with the direction. The wave parameters were calculated from the first moment, second moment, and even higher moments of the spectrum.

The formula for calculating the significant wave height is as follows [30]:

$$H_s = 4\sqrt{m_0} = 4\sqrt{\int S(\omega)\mathrm{d}\omega} \tag{12}$$

The calculation formula of the inversion of mean zero-crossing period is as follows, which is calculated from the 0th and 2nd moments [31].

$$T_Z = 2\pi\sqrt{\frac{m_0}{m_2}} = 2\pi\sqrt{\frac{\int S(\omega)\mathrm{d}\omega}{\int \omega^2 S(\omega)\mathrm{d}\omega}} \tag{13}$$

We integrated the optimal wave spectrum obtained from the inversion of each sub-image and calculated the wave parameters. Each scene data could obtain 400 calculation results of significant wave height and zero-crossing period parameters. Then, we compared them with the matching wave information provided by ERA-Interim to calculate the root mean square error. Therefore, the accuracy of the inversion of sea wave information by the E spectrum and PM spectrum as the first guess spectrum could be compared.

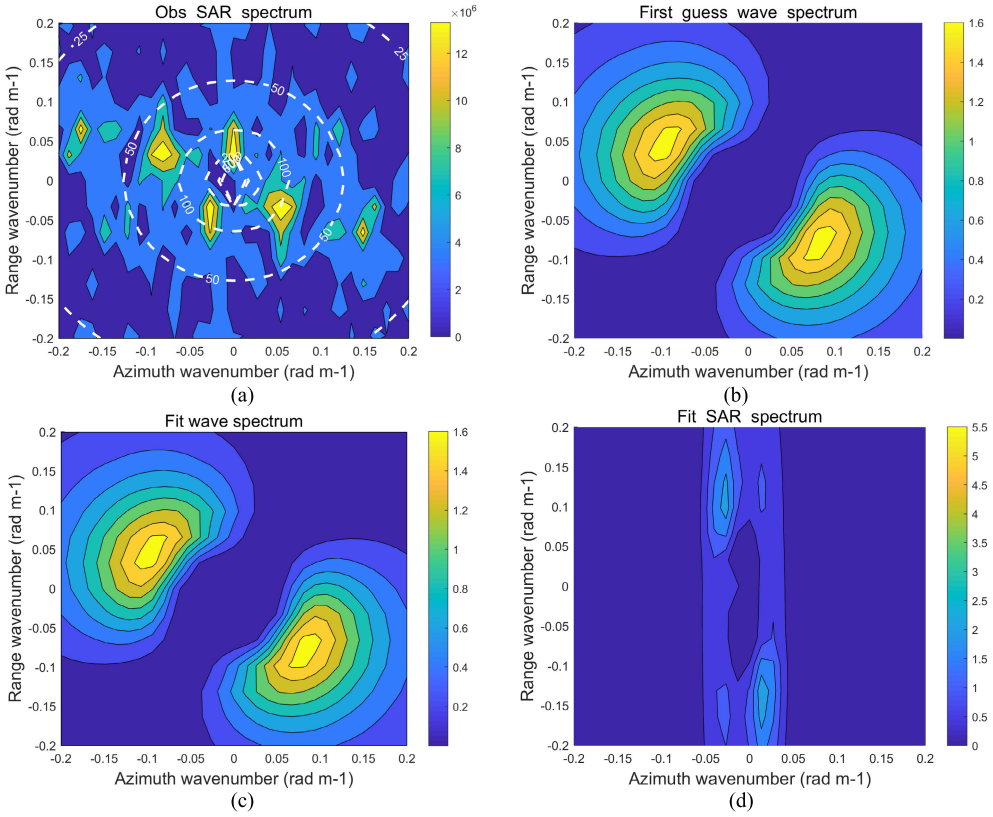

FIGURE 9. Wave spectrum inversion results of 09-JUL-2019 11:45:39 (UTC) SENTINEL-1A SAR data when the E spectrum was used as the first guess spectrum (a. Observed SAR spectrum; b. First guess spectrum (E spectrum); c. Fit wave spectrum; d. Fit SAR spectrum).

Table.1 shows the root mean square error (RMSE) of the comparison between the wave parameters inversion results obtained from all 16 scenes SAR images and the wave information provided by ERA-Interim. Figs 11-12 show the wave parameter distribution map obtained from the inversion of 25-JUL-2012 22:07:39 (UTC) RADARSAT-2 SAR data and 09-JUL-2019 11:45:39 (UTC) SENTINEL-1A SAR data.

From Table.1, it was found by comparison that the accuracy of the zero-crossing wave period inversion results of the PM spectrum and E spectrum as the first guess spectrum was not much different. The difference of total RMSE was about 0.1s. Therefore, this paper focused on the inversion results of significant wave height.

The significant wave height (H_S) is the most important wave parameter, and the inversion result of the significant wave height largely depends on the accuracy of the first guess spectrum [32]. The significant wave height reflects the common contribution of wind waves and swells. Therefore, the accuracy of the significant wave height inversion results is an important factor for the applicability of the wave spectra.

First, in Table.1, the mostly inversion results with the E spectrum as the first guess spectrum met the inversion accuracy requirements recognized in the field of SAR wave parameter inversion (H_S RMSE$<$ 0.5m; T_Z RMSE $<$1.2 s).

Then, the inversion result of PM spectrum as the first guess spectrum was usually worse than that of E spectrum. And the significant wave height RMSE of some data were greater than 0.5 m, as shown in results 1, 3, 4, and 11. These bad results were all under the situation that the average wind speed on the sea surface was higher than 9m/s.

The total significant wave height RMSE showed that the inversion result of the E spectrum as the first guess spectrum was more accurate. Thus, the E spectrum had the ability to be used as the first guess spectrum to invert the wave spectrum of the measured SAR data.

In order to understand the influence of sea surface wind speed and sea state on the accuracy of the inversion results, we segmented all images according to wind speeds and significant wave heights.

Each scene SAR image can get 400 sub-images. Each sub-image data was inverted separately, and 6198 effective inversion results were obtained. We calculated these inversion results according to the 10m wind speed and significant wave height provided by ERA-Interim. The statistics of the number of data between 5m/s - 13 m/s wind speeds and 0.5 m - 3.5 m wave heights were shown in the Fig. 13.

Then we obtained the RMSE between the significant wave height inversion results and ERA-Interim data in each range. The comparison results in different ranges were shown

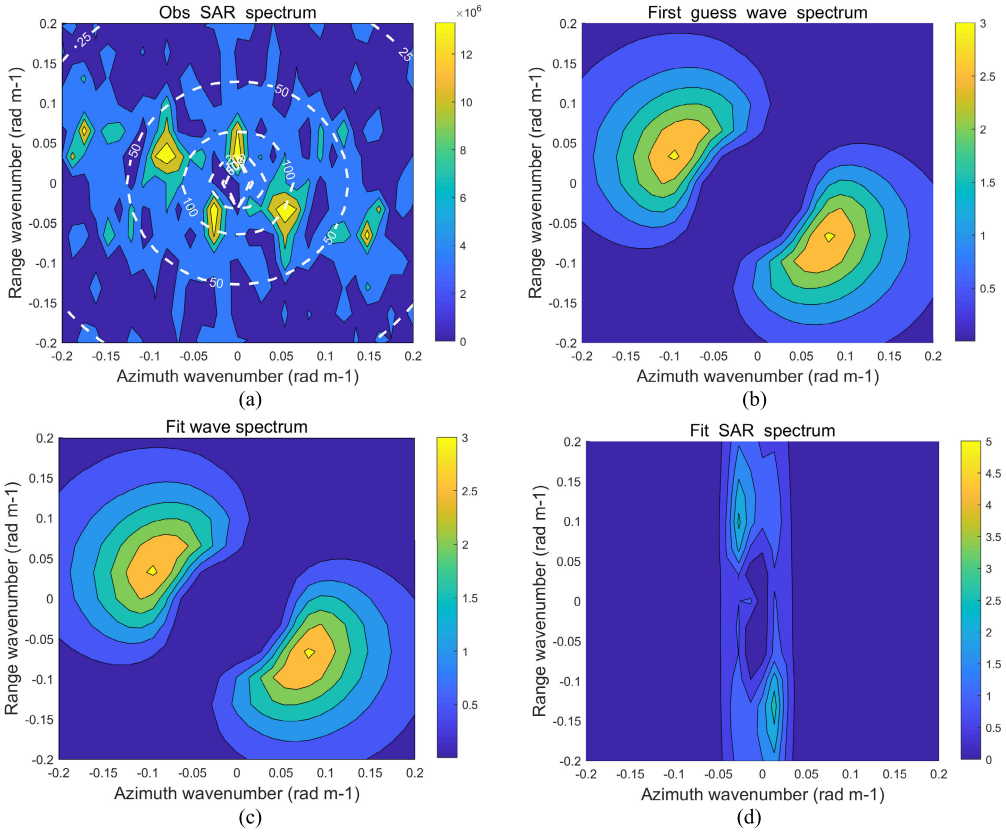

FIGURE 10. Wave spectrum inversion results of 09-JUL-2019 11:45:39 (UTC) SENTINEL-1A SAR data when the PM spectrum was used as the first guess spectrum (a. Observed SAR spectrum; b. First guess spectrum (PM spectrum); c. Fit wave spectrum; d. Fit SAR spectrum).

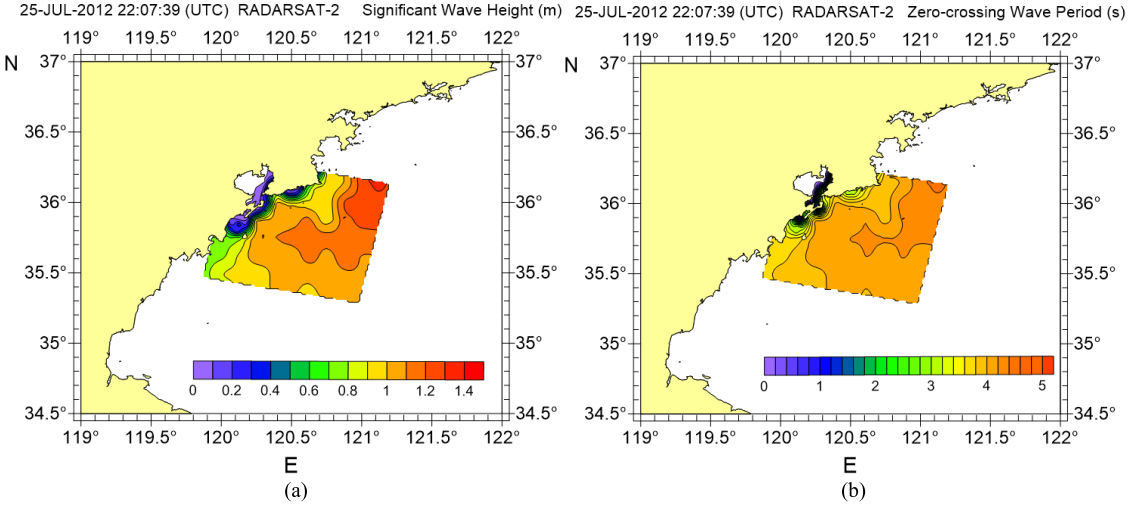

FIGURE 11. The wave parameter distribution map obtained from the inversion of 25-JUL-2012 22:07:39 (UTC) RADARSAT-2 SAR data (a. Significant wave height; b. Zero-crossing wave period).

in Tables.2-3. The trend of the inversion results in different ranges is shown in Figure 14. From these results, we can analyze the applicability of E spectrum and PM spectrum as the first guess spectrum under different significant wave heights and wind speeds.

In the comparison results at different wind speeds, we can see that the RMSE of the inversion of the E spectrum and PM spectrum as the first guess spectrum gradually increased with wind speeds increasing. Among them, when the wind speed was between 5 m/s - 9 m/s, both the E

TABLE 1. Comparison of the wave parameters inversion results with ERA-Interim wave parameters.

Serial number	Satellite type	SAR imaging time(UTC)	Average wind speed (10 m wind speed) (m/s)	Significant wave height range(m)	Input first guess spectrum	RMSE	
						H_S(m)	T_Z(s)
1	SENTINEL-1A	08-JUN-2018 11:45:14	10.27	2.01 - 2.20	PM	1.2389	0.3435
					E	0.4168	0.0760
2	SENTINEL-1A	02-JUL-2019 11:45:15	6.91	0.99 - 1.17	PM	0.4782	0.8286
					E	0.2103	0.9952
3	SENTINEL-1A	07-AUG-2019 11:45:18	11.70	2.01 - 2.35	PM	2.1105	0.6879
					E	0.9855	0.3861
4	SENTINEL-1A	19-AUG-2019 11:45:18	10.09	1.90 - 2.21	PM	1.1973	0.3005
					E	0.4280	0.3291
5	SENTINEL-1A	23-MAR-2019 11:45:31	5.19	0.89 - 1.01	PM	0.1591	0.6223
					E	0.1083	0.7440
6	SENTINEL-1A	03-JUN-2019 11:45:20	7.51	1.61 - 2.09	PM	0.2696	0.9336
					E	0.4812	1.1102
7	SENTINEL-1A	15-JUN-2019 11:45:20	8.26	1.51 - 1.89	PM	0.4547	0.2858
					E	0.1106	0.4188
8	SENTINEL-1A	27-JUN-2019 11:45:21	7.57	1.52 - 2.06	PM	0.2519	0.8223
					E	0.3498	0.9664
9	SENTINEL-1A	09-JUL-2019 11:45:39	7.86	1.41 - 1.87	PM	0.3186	0.7256
					E	0.1650	0.8849
10	SENTINEL-1A	21-JUL-2019 11:45:23	8.01	1.44 - 2.15	PM	0.3797	0.4948
					E	0.1965	0.6657
11	SENTINEL-1A	26-AUG-2019 11:45:25	9.91	1.99 - 2.45	PM	0.9347	0.3742
					E	0.2296	0.2627
12	SENTINEL-1A	07-SET-2019 11:45:20	7.74	1.41 - 1.85	PM	0.3135	0.3830
					E	0.1834	0.5294
13	SENTINEL-1A	03-AUG-2019 09:07:57	10.42	2.79 - 2.88	PM	0.6064	0.4335
					E	0.2584	0.6627
14	SENTINEL-1A	03-AUG-2019 09:08:12	10.99	3.27 - 3.31	PM	0.5427	0.4982
					E	0.4631	0.7806
15	RADARSAT -2	25-JUL-2012 22:07:39	6.29	0.22 - 1.00	PM	0.3764	0.8354
					E	0.1336	0.8097
16	RADARSAT -2	23-JUN-2019 21:53:25	5.25	0.87 - 0.91	PM	0.3928	0.7966
					E	0.2805	0.7565
Total					PM	0.8048	0.5948
					E	0.3832	0.6903

spectrum and the PM spectrum as the first guess spectrum had good inversion effects. When the wind speed was greater than 9m/s, the accuracy of the inversion results of the PM spectrum as the first guess spectrum began to fail to meet the requirements. When the wind speed was greater than 11m/s, the accuracy of the inversion results of the E spectrum as the first guess spectrum was gradually unable to meet the requirements, but it was still better than that of the PM spectrum.

In the comparison results at different significant wave heights, we can see that when the wave height was less than 2m, the two spectra as the first guess spectrum had good inversion effects. When the wave height was between 2.0 m - 2.5 m, the RMSE of the E spectrum as the first guess spectrum was 0.5834, and that of the PM spectrum was 1.3787. The inversion accuracy of the two spectra as the first guess spectrum cannot meet the requirements, but the inversion results of the E spectrum as the first guess spectrum was obviously more accurate than that of the PM spectrum. When the wave height was higher than 2.5 m, the inversion accuracy of the PM spectrum as the first guess spectrum cannot meet the requirements. On the contrary, the inversion

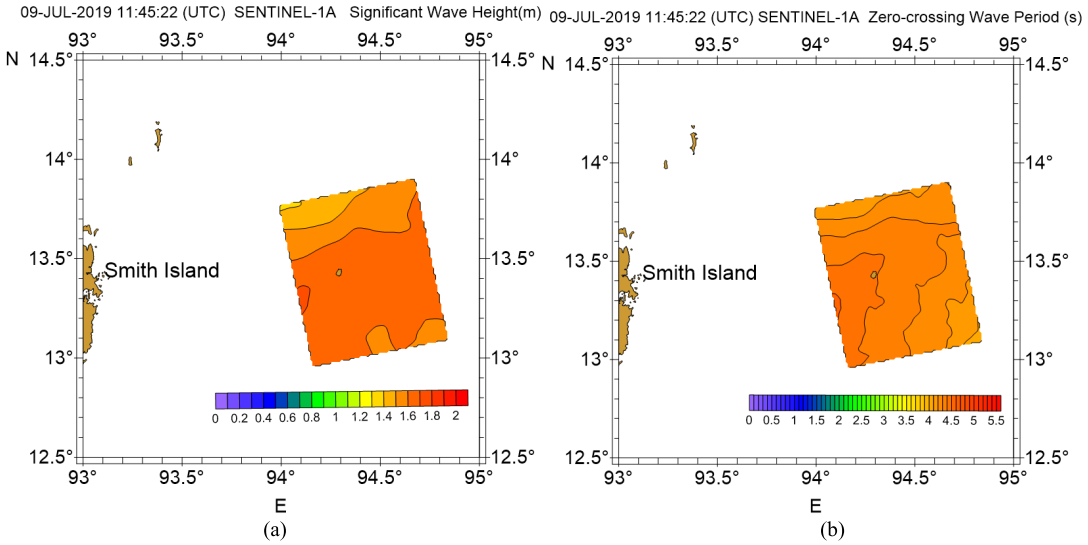

FIGURE 12. The wave parameter distribution map obtained from the inversion of 09-JUL-2019 11:45:39 (UTC) SENTINEL-1A SAR data (a. Significant wave height; b. Zero-crossing wave period).

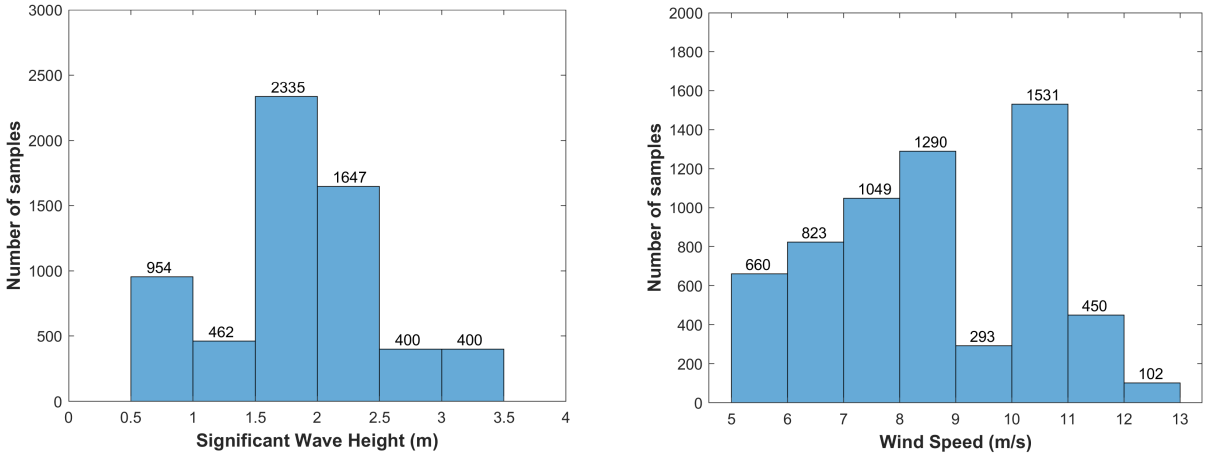

FIGURE 13. Number of SAR sub-images data at different significant wave heights and wind speeds.

TABLE 2. The H_S comparison results at different wind speeds.

Wind speed range (m/s)	RMSE	
	E spectrum	PM spectrum
5 - 6	0.2337	0.1615
6 - 7	0.3154	0.4287
7 - 8	0.3027	0.2357
8 - 9	0.1598	0.4007
9 - 10	0.1761	0.8370
10 - 11	0.3903	1.0104
11 - 12	0.7630	1.6210
12 - 13	1.2458	2.4855

accuracy of the E spectrum as the first guess spectrum all met the requirements.

It can be seen from the above analysis that the E spectrum as the first guess spectrum had a good inversion effect

TABLE 3. The H_S comparison results at different significant wave heights.

Significant wave height range(m)	RMSE	
	E spectrum	PM spectrum
0.5 - 1	0.2074	0.2588
1 - 1.5	0.2011	0.4635
1.5 - 2	0.2757	0.4419
2 - 2.5	0.5834	1.3787
2.5 - 3	0.2584	0.6064
3 - 3.5	0.4631	0.5427

under moderate wind speed conditions, but as the wind speed increased, the accuracy of the inversion results would decrease. At the same time, the E spectrum had a good inversion effect as the first guess spectrum in the researched wave height ranges, so that the E spectrum was suitable for inversion as the first guess spectrum at medium sea conditions.

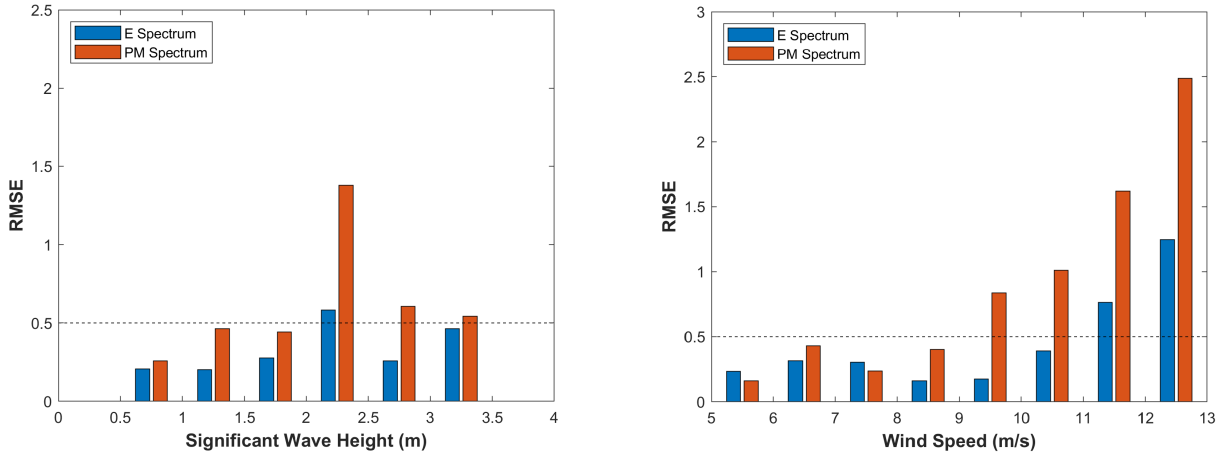

FIGURE 14. The H_S comparison results at different significant wave heights and wind speeds.

The PM spectrum as the first guess spectrum had a good inversion effect when the wave height was less than 2 m, but the inversion effect was not good when the wave height was greater than 2 m and the wind speed was higher than 9 m/s. This confirmed that the PM spectrum was suitable for inversion under the low sea state and low wind speed, specifically when the wave height was lower than 2m and the wind speed was lower than 9 m/s.

The analysis of the inversion results showed that the inversion effect of the E spectrum as the first guess spectrum was better than that of the PM spectrum. That was because, as a full wavenumber spectrum, the E spectrum added a description of ocean waves in the high wavenumber domain, which was not available in the PM spectrum.

In addition, combined with the above analysis of E spectrum and PM spectrum S(k) for the different wind speeds (Fig.6), we can see that when the sea surface wind speed was greater than 9m/s, the E-spectrum contained a wider high wave number domain to obtain more wave information. Therefore, the inversion effect of E spectrum as the first guess spectrum would be better than that of PM spectrum. The inversion results also proved this conclusion.

In summary, by analyzing the inversion results of SENTINEL-1A and RADARSAT-2 SAR satellite data, we can see that the ability of the E spectrum as the first guess spectrum to invert sea wave parameters was better than that of the PM spectrum. Therefore, the E spectrum was more suitable as the first guess spectrum for SAR wave spectrum inversion. That is, the E spectrum was the best first guess spectrum model for SAR wave spectrum inversion.

V. CONCLUSION

Based on the SENTINEL-1A and RADARSAT-2 SAR satellite data, this paper systematically evaluated the ability of the E spectrum and PM spectrum as the first guess spectrum to retrieve the wave spectrum by MPI method. The significant wave height and zero-crossing period wave parameters obtained from SAR inversion were compared with ECMWF wave data, and the applicability of the PM spectrum and E spectrum as the first guess spectrum to invert the wave spectrum and wave parameters was analyzed. The results provided an important reference for the application of SAR in the monitoring of the Maritime Silk Road. The conclusions are as follows:

(1) The E spectrum as the first guess spectrum of the MPI method had a good effect on the inversion of the wave spectrum. The inversion of the wave parameters with the E spectrum as the first guess spectrum had good consistency with the ECMWF data, indicating that the E spectrum was suitable as the first guess spectrum for the SAR wave spectrum inversion. But as the wind speed increased, especially when the wind speed was greater than 11m/s, the accuracy of the inversion would decrease. Additionally, the E spectrum was a full wavenumber spectrum, so the E spectrum used as the first guess spectrum for inversion obtained more complete wave information.

(2) The PM spectrum was suitable for inversion as the first guess spectrum under low sea conditions and wind speeds, specifically when the significant wave height was lower than 2m and the wind speed was lower than 9m/s. Therefore, the E spectrum was more suitable as the first guess spectrum for SAR wave spectrum inversion under different sea conditions and inversion of various types of waves. The E spectrum was the best first guess spectrum model for SAR wave spectrum inversion.

REFERENCES

[1] S. Bi, L. Zhang, Y. Gu, H. Wang, L. Wen, T. Li, and J. P. Bi, "Analysis of the changes of ports and port-city relationships along the 21st-century maritime silk road," (in Chinese), *J. Univ. Chin. Acad. Sci.*, vol. 37, no. 1, pp. 74–82, 2020.

[2] H. Wang, H. Liu, Y. F. Zhang, T. Y. Zhang, and X. Ren, "Risk prevention of marine and meteorological disasters along the '21st century maritime silk road,"' (in Chinese), *Chin. Sci. Bull.*, vol. 65, no. 06, pp. 453–462, 2020.

[3] C. W. Zheng, J. J. Xu, C. Zhan, and Q. Wang, *21st Century Maritime Silk Road: Wave Energy Resource Evaluation*. Singapore: Springer, 2019.

[4] C. W. Zheng, C. Y. Li, H. L. Wu, and M. Wang, *21st Century Maritime Silk Road: Construction of Remote Islands and Reefs*. Singapore: Springer, 2018.
[5] C.-W. Zheng, Y.-G. Chen, C. Zhan, and Q. Wang, "Source tracing of the swell energy: A case study of the pacific ocean," *IEEE Access*, vol. 7, pp. 139264–139275, 2019.
[6] C. Zheng, B. Liang, X. Chen, G. Wu, X. Sun, and J. Yao, "Diffusion characteristics of swells in the north indian ocean," *J. Ocean Univ. China*, vol. 19, no. 3, pp. 479–488, Jun. 2020.
[7] J. C. Wang and Y. Z. Li, "Development and application of ocean data buoy technology in China," (in Chinese), *Shandong Sci.*, vol. 32, no. 5, pp. 1–20, 2019.
[8] Y. Q. Qi, P. C. Chu, and P. Shi, "Analysis of significant wave heights from WWATCH and TOPEX/Poseidon altimetry," (in Chinese), *J. Ocean*, vol. 25, no. 4, pp. 1–9, 2003.
[9] Y. X. Cheng and L. F. Yuan, "Development status of spaceborne synthetic aperture radar," (in Chinese), *Electron. Test*, vol. 343, no. 8, pp. 145–146, 2016.
[10] W. J. Plant and L. M. Zurk, "Dominant wave directions and significant wave heights from synthetic aperture radar imagery of the ocean," *J. Geophys. Res., Oceans*, vol. 102, no. C2, pp. 3473–3482, Feb. 1997.
[11] K. Hasselmann and S. Hasselmann, "On the nonlinear mapping of an ocean wave spectrum into a synthetic aperture radar image spectrum and its inversion," *J. Geophys. Res.*, vol. 96, no. C6, p. 10713, 1991.
[12] Y. J. He, "Parametric method for synthetic aperture radar to extract ocean wave direction spectrum," (in Chinese), *Sci. Bull.*, vol. 4, pp. 94–99, 1999.
[13] C. Mastenbroek and C. F. de Valk, "A semiparametric algorithm to retrieve ocean wave spectra from synthetic aperture radar," *J. Geophys. Res., Oceans*, vol. 105, no. C2, pp. 3497–3516, 2000.
[14] G. Engen and H. Johnsen, "SAR-ocean wave inversion using image cross spectra," *IEEE Trans. Geosci. Remote Sens.*, vol. 33, no. 4, pp. 1047–1056, Jul. 1995.
[15] J. Schulz-Stellenfleth, S. Lehner, and D. Hoja, "A parametric scheme for the retrieval of two-dimensional ocean wave spectra from synthetic aperture radar look cross spectra," *J. Geophys. Res., Oceans*, vol. 110, no. C5, May 2005, Art. no. C05004.
[16] S. Zhu, W. Shao, M. Armando, J. Shi, J. Sun, X. Yuan, J. Hu, D. Yang, and J. Zuo, "Evaluation of chinese quad-polarization Gaofen-3 SAR wave mode data for significant wave height retrieval," *Can. J. Remote Sens.*, vol. 44, no. 6, pp. 588–600, Nov. 2018.
[17] B. Lin, *A Study of Ocean Wave Parameters Retrieved From C-Band Sentinel-1 SAR Images*. Zhoushan, China: Zhejiang Ocean Univ., 2018.
[18] J. Sun, *The Retrievement of Ocean Wave Information From SAR Images*. Qingdao, China: Ocean Univ. China, 2005.
[19] W. J. Pierson and L. Moskowitz, "A proposed spectral form for fully developed wind seas based on the similarity theory of S. A. kitaigorodskii," *J. Geophys. Res.*, vol. 69, no. 24, pp. 5181–5190, Dec. 1964.
[20] D. E. Hasselmann, M. Dunckel, and J. A. Ewing, "Directional wave spectra observed during JONSWAP 1973," *J. Phys. Oceanogr.*, vol. 10, no. 8, pp. 1264–1280, Aug. 1980.
[21] X. M. Li, *Research on the Wave Inversion Algorithm of ENVISAT Satellite ASAR Wave Model Data*. Qingdao, China: Ocean Univ. China, 2010.
[22] T. Elfouhaily, B. Chapron, K. Katsaros, and D. Vandemark, "A unified directional spectrum for long and short wind-driven waves," *J. Geophys. Res., Oceans*, vol. 102, no. C7, pp. 15781–15796, Jul. 1997.
[23] D. Geudtner, R. Torres, P. Snoeij, M. Davidson, and B. Rommen, "Sentinel-1 system capabilities and applications," in *Proc. IEEE Geosci. Remote Sens. Symp.*, Quebec City, QC, Canada, Jul. 2014, pp. 1457–1460.
[24] W. M. Moon, G. Staples, D.-J. Kim, S.-E. Park, and K.-A. Park, "RADARSAT-2 and coastal applications: Surface wind, waterline, and intertidal flat roughness," *Proc. IEEE*, vol. 98, no. 5, pp. 800–815, May 2010.
[25] X. J. Xu and X. F. Li, *Radar Phenomenological Models for Ships on Time Evolving Sea Surface*. Beijing, China: Nat. Defense Ind. Press, 2013, pp. 5–6.
[26] P. A. Hwang, S. Atakturk, A. Sletten, and D. B. Trizna, "A study of the wavenumber spectra of short water waves in the ocean," *J. Phys. Oceanogr.*, vol. 26, no. 7, pp. 1266–1285, Jul. 1996.
[27] O. M. Phillips, "Spectral and statistical properties of the equilibrium range in wind-generated gravity waves," *J. Fluid Mech.*, vol. 156, no. 1, pp. 505–531, 1985.
[28] G. Luo, *Research on Nonlinear Electromagnetic Scattering Characteristics of Ocean Waves*. Xi'an, China: Xidian University, 2015.
[29] L. B. Wang and Q. Feng, "Directional ocean wave spectrum from SAR image using Hasselmann's methods," *Chin. J. Radio Sci.*, vol. 19, no. 1, pp. 67–71, 2004.
[30] M. S. Longuet-Higgins, "The statistical analysis of a random, moving surface," *Philos. Trans. Roy. Soc. London. A, Math. Phys. Sci.*, vol. 249, no. 966, pp. 321–387, 1957.
[31] M. S. Longuet-Higgins, "On the joint distribution of the periods and amplitudes of sea waves," *J. Geophys. Res.*, vol. 75, no. 33, pp. 2688–2694, 1975.
[32] F. Hua, B. Fan, Y. Lu, and J. Q. Wang, "An empirical relationship between the peak period of the ocean wave spectrum and the zero-crossing period," *Adv. Mar. Sci.*, vol. 1, pp. 16–20, 2004.

YONG WAN received the B.S. degree in application electronic technology and the M.S. degree in control theory and control engineering from the China University of Petroleum, Dongying, China, in 2001 and 2004, respectively, and the Ph.D. degree in marine information detection and processing from the Ocean University of China, Qingdao, China, in 2015.

Since 2019, he has been an Associate Professor with the China University of Petroleum, Qingdao. His research interests include marine information detection and processing, SAR detection for ocean wave and wind, wave energy, and wind energy assessment.

RUOZHAO QU received the bachelor's degree from Shandong Agricultural University, Taian, China, in 2019. He is currently pursuing the master's degree with the China University of Petroleum. His research interests include marine information detection and processing and SAR detection for ocean wave.

YONGSHOU DAI received the B.S. degree in automation professional from the China University of Petroleum, Dongying, China, in 1986, the M.S. degree in computer application from Northern Jiaotong University, Beijing, China, in 1992, and the Ph.D. degree in control theory and control engineering from the Beijing University of Science and Technology, Beijing, in 2007. He is currently engaged in the teaching and research of marine information detection and processing with the College of Oceanography and Space Informatics, China University of Petroleum, Qingdao, China.

XIAOYU ZHANG received the bachelor's degree from Yantai University, Yantai, China, in 2017, and the master's degree from the China University of Petroleum, Qingdao, China, in 2020. Her research interests include marine information detection and processing and SAR detection for ocean wave.